
Controllable diffusion-based generation for multi-channel biological data

Haoran Zhang

University of Texas at Austin
Austin, TX 78712
hz6453@utexas.edu

Mingyuan Zhou

University of Texas at Austin
Austin, TX 78712
mingyuan.zhou@mcombs.utexas.edu

Wesley Tansey

Memorial Sloan Kettering Cancer Center
New York, NY 10065
tanseyw@mskcc.org

Abstract

Spatial profiling technologies in biology, such as imaging mass cytometry (IMC) and spatial transcriptomics (ST), generate high-dimensional, multi-channel data with strong spatial alignment and complex inter-channel relationships. Generative modeling of such data requires jointly capturing intra- and inter-channel structure, while also generalizing across arbitrary combinations of observed and missing channels for practical application. Existing diffusion-based models generally assume low-dimensional inputs (e.g., RGB images) and rely on simple conditioning mechanisms that break spatial correspondence and ignore inter-channel dependencies. This work proposes a unified diffusion framework for controllable generation over structured and spatial biological data. Our model contains two key innovations: (1) a hierarchical feature injection mechanism that enables multi-resolution conditioning on spatially aligned channels, and (2) a combination of latent-space and output-space channel-wise attention to capture inter-channel relationships. To support flexible conditioning and generalization to arbitrary subsets of observed channels, we train the model using a random masking strategy, enabling it to reconstruct missing channels from any combination of inputs. We demonstrate state-of-the-art performance across both spatial and non-spatial prediction tasks, including protein imputation in IMC and gene-to-protein prediction in single-cell datasets, and show strong generalization to unseen conditional configurations.

1 Introduction

Recent advances in generative models enable structured generation, prediction, and imputation across various data domains [1, 2]. Specifically, diffusion models have shown a remarkable capacity for generating high-fidelity samples with corrupted data or conditionals like text prompts, especially in natural images and language generation tasks. However, the domain of biological profiling data, including imaging mass cytometry (IMC) [3], spatial transcriptomics (ST) [4], and other biological profiling technologies, poses unique structural challenges that remain underexplored.

A key characteristic of biological profiling data is its many-channel nature, where each dataset comprises a substantial number of channels ($n \geq 30$ for proteomics technologies and $n \geq 1000$ for transcriptomics technologies). For instance, in spatial profiling data, each channel designates a specific molecule of interest (e.g., proteins and genes), and each pixel (or cell) represents a spatially co-registered vector of biologically distinct signals. Unlike RGB images with fixed and highly correlated

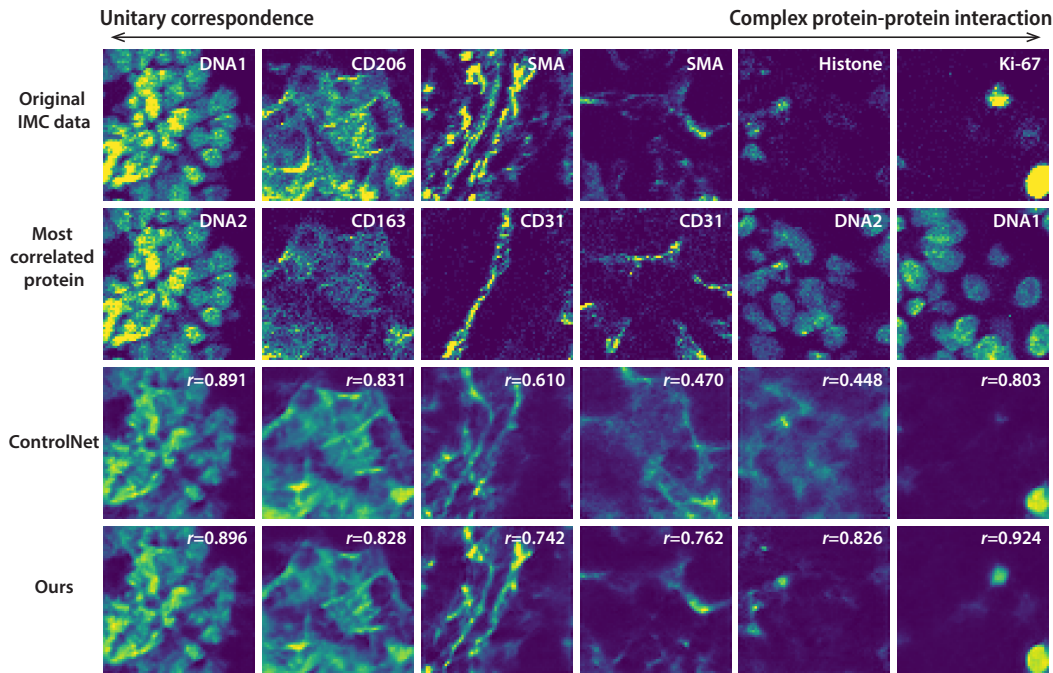


Figure 1: Visual comparison of samples generated by our model with samples generated by ControlNet-style counterpart. Without the channel attention modules and attention injection mechanisms, ControlNet-style generative models can handle simple channels with unitary inter-channel correlation, like DNA1 (the right-most column), but easily fail in the ones like tumor markers that have more complex protein-protein interaction like Ki-67 and α SMA (columns 3-6).

channels, biological channels often have complex and variable inter-channel correlations. More importantly, in practice, many channels may be unobserved due to technical limitations, acquisition constraints, or experimental design. This constraint forces biologists to decide which signals are most important to measure before even seeing the data, limiting the scope and breadth of insights gained from an experiment. A generative framework that can handle high-dimensional biological profiling data, maintain spatial alignment, accommodate missing channels, and model diverse inter-channel relationships could potentially fill in missing channels. Such a method would enhance the scope of biological studies and potentially lead to more scientific discoveries.

This problem is more complex than conditional natural image generation. The conditioning inputs in this task are not abstract prompts (e.g., text or class labels), but observed channels of the same sample. These conditions are spatially aligned with the target, and such spatial alignment should be preserved throughout the generation process. Naive conditioning mechanisms, such as global embeddings and flat concatenation, break spatial correspondence, making them incompatible with biological profiling tasks. On the other hand, the number of channels is large and their interactions are highly context-dependent. Some channels co-localize only within specific spatial niches or cell types; others may be mutually exclusive. Therefore, modeling such sparse, nonlinear, and asymmetric dependencies requires a generative framework that maintains spatial alignment and adapts to diverse and context-dependent channel semantics in biological data.

Existing data imputation and colorization methods, including score-based [5] and conditional diffusion models [6], offer powerful tools for spatially constrained image generation. However, these methods are tailored to low-dimensional RGB images and use generic conditioning strategies that ignore channel semantics. ControlNet [2] and BrushNet [7] introduce multiscale spatial conditioning mechanisms but remain limited to low-dimensional RGB-like inputs and rely on pre-trained diffusion models, which do not model inter-channel relationships in a principled way. As a result, such methods fail to generalize to the high-dimensional setting of biological data, where conditional generalization and principled modeling of inter-channel relationships are important.

In this work, we introduce a diffusion-based generative model for controllable multi-channel data generation with strong spatial alignment but heterogeneous channel semantics. We demonstrate its performance and generalizability in tasks of generating biological profiling data with subsets of observable channels. Our method handles arbitrary combinations of observed and missing channels, maintains spatial alignment, and captures complex inter-channel dependencies. To achieve this, we propose three key components: (1) a hierarchical feature injection mechanism that conditions the generation of multi-resolution spatial features on the observed channels, preserving alignment and enabling fine-grained control, (2) a combination of latent- and output-space channel-wise attention to explicitly model semantic relationships between channels during generation, and (3) a random masking training strategy that amortizes over the conditional space and enables dynamic test time conditioning. Together, these components allow our model to generate multi-channel biological profiling data with high fidelity across resolution scales within a unified diffusion framework. Our model achieves state-of-the-art results in both spatial and non-spatial settings and supports test-time controllability over arbitrary conditioning on subsets of channels.

2 Background

2.1 Diffusion models

Diffusion models are a class of generative models that approximates the data distribution by modeling the gradient of its log-density (score function) [5]. This is achieved by coupling a forward process that progressively perturbs the data with a reverse process that learns to undo this perturbation. The forward process transforms data \mathbf{x}_0 into a noise distribution \mathbf{x}_T over T timesteps by injecting noise from a known distribution like a Gaussian [8],

$$q(\mathbf{x}_t | \mathbf{x}_0) = \mathcal{N}(\mathbf{x}_t | \sqrt{\alpha_t}\mathbf{x}_0, (1 - \alpha_t)\mathbf{I}), \quad (1)$$

where α_t is a noise schedule parameterizing the variance at each timestep t . As t approaches T , the data distribution converges to a simple prior, such as a standard Gaussian. The reverse process reconstructs data from noise by learning to reverse the corruption introduced during the forward process. This is achieved through a neural network $\epsilon_\theta(x_t, t)$, trained to predict the noise ϵ added at each timestep [9]. The denoising process is guided by the objective:

$$\mathcal{L}_{\text{DDPM}} = \mathbb{E}_{\mathbf{x}_0, \epsilon, t} [\|\epsilon - \epsilon_\theta(\mathbf{x}_t, t)\|^2], \quad (2)$$

where $\epsilon \sim \mathcal{N}(0, \mathbf{I})$ is the Gaussian noise injected by the forward process. By minimizing this objective, the model learns to reconstruct x_0 from the noisy x_t at any timestep t . This denoising approach is deeply connected to score matching. Specifically, the noise prediction $\epsilon_\theta(x_t, t)$ can be used to compute the gradient of the log-density (score function) as:

$$\nabla_{\mathbf{x}_t} \log q(\mathbf{x}_t) \propto -\frac{\epsilon_\theta(\mathbf{x}_t, t)}{\sqrt{1 - \alpha_t}} \quad (3)$$

Thus, accurately predicting the noise is equivalent to estimating the score function $\nabla_{\mathbf{x}_t} \log q(\mathbf{x}_t)$, which guides the reverse process. This insight bridges denoising and score matching, making the reverse process a refinement procedure that progressively moves noisy samples back to the data manifold [5].

2.2 Structured multi-channel imputation

Image imputation is a classical problem in computer vision and generative modeling, where the objective is to recover missing or corrupted parts of an image given the observed context. Formally, given an observation c , classical imputation methods aim to estimate the full image x by modeling the conditional distribution $p(x | c)$. This problem has been extensively studied in the context of RGB images, where $x, v \in \mathbb{R}^{3 \times H \times W}$, and inpainting primarily relies on spatial continuity within the image domain [10].

We generalize this problem to the setting of structured multi-channel data, where each channel corresponds to a semantically distinct measurement—such as a spectral band, a protein marker, or a gene expression. Let $c \in \mathbb{R}^{C_o \times H \times W}$ denote the observed data, and let $x \in \mathbb{R}^{C \times H \times W}$ denote the full data, where $C = C_o + C_m \geq 1$, $C_o \geq 1$, and $C_m \geq 0$ denote the number of total, observed, and

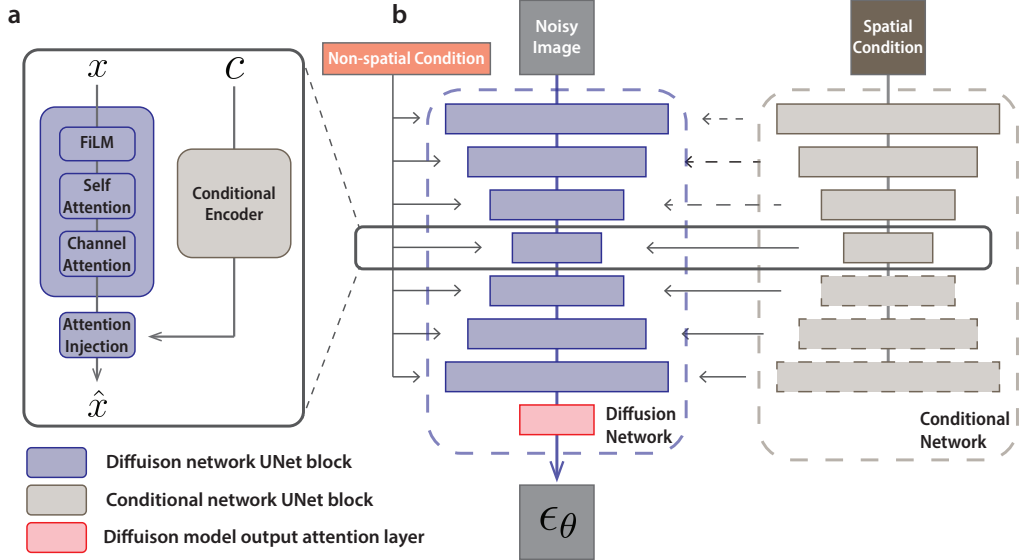


Figure 2: Overview of the proposed diffusion model for multi-channel data generation. (a) Custom channel-wise attention: UNet Block with channel attention module that models the inter-channel relationships. (b) Hierarchical feature injection: a parallel conditional network encodes the spatial condition, producing features at different resolution that are injected into the corresponding UNet block in the diffusion network.

missing channels respectively. Note that when $C_m = 0$ and $C_o = C = 3$, this formulation reduces to the classical RGB image imputation problem ($C = 1$ for the grayscale case), and when $C_m = 3$ and $C_o = 1$, it reduces to the classical RGB image colorization problem.

This general formulation applies across a broad range of problems at different resolution. When $H = W = 1$, the input reduces to a high-dimensional vector, making this formulation applicable to non-spatial data imputation such as single-cell data, where one may predict single cell protein expression from single-cell RNA (scRNA) sequencing data. When $H, W > 1$, the formulation supports spatially structured imaging tasks such as IMC channel prediction, where local morphology and global tissue organization both contribute to the reconstruction target.

3 Methods

We propose a diffusion-based generative framework for multi-channel biological data conditioned on arbitrary subsets of observed channels. Let $x \in \mathbb{R}^{C \times H \times W}$ be the data with a full set of channels and $c \in \mathbb{R}^{C_o \times H \times W}$ the observed subset. Our goal is to learn the conditional distribution $p(x|c)$, where x and c are spatially aligned.

3.1 Spatially Aligned Feature Injection for Structured Conditioning

We first introduce a hierarchical feature injection mechanism that conditions x on multi-resolution representations of the observed c . We employ two jointly trained parallel networks: a diffusion network that processes the noisy target x_t , and a contextual network that processes the observed spatial condition c . At each resolution level ℓ , the diffusion network encodes x_t to $D_\ell(x_t)$, and the contextual network gives the contextual feature map $E_\ell(c)$, which is injected into the corresponding layer of the diffusion network (fig. 2b). These contextual features are injected through a channel-wise gating module:

$$z_\ell = D_\ell(x_t) + \text{SE}(E_\ell(c)) \quad (4)$$

allowing for the flexible injection of spatial conditions. The $\text{SE}(\cdot)$ is the Squeeze-and-Excitation block that serves as soft channel attention (see section 3.3 for detail) and selectively injects the condition while the spatial alignment is preserved. This design allows the model to condition not

just on a fixed global representation of c but on a series of contextual features $\{E_\ell(c)\}_{\ell=1}^L$ that vary across resolution. This setup reflects the intuition that certain patterns in x , e.g. global motifs versus local structures, may depend on different aspects of c . Early encoder layers focus more on the local structures, while late layers draw high-level, global structures.

3.2 Training with Random Channel Masking

Different experiments may measure different subsets of possible channels. Rather than training separate models to predict individual channels, our goal is to produce full multi-channel outputs (i.e. the complete protein panel). Constructing our model so that it can condition on any subset enables us to train across multiple datasets and flexibly apply our model on each. To create a unified model, we propose a random channel masking strategy during training. In each iteration, we randomly sample a subset of channels $S_o \subset \{1, \dots, C\}$ as observed, and mask out the remaining $S_m = \{1, \dots, C\} \setminus S_o$. The masked subset x_{S_m} is zeroed out in spatial condition c , and the model reconstructs the full panel $x \in \mathbb{R}^{C \times H \times W}$.

Randomly varying S_o during training encourages the model to learn conditional generation under diverse partial contexts. As a result, the trained model can generalize to arbitrary combinations of observed and missing channels at the test time, including unseen configurations. At the same time, because the model always predicts all channels, it avoids the need for channel-specific heads or separate training for each protein, and enables comprehensive downstream analysis and one-stop training.

Algorithm 1 Random Channel Masking

Require: Full data $x \in \mathbb{R}^{C \times H \times W}$, masking prob. p

- 1: **for** each training iteration **do**
- 2: Sample observed set $S_o \subset \{1, \dots, C\}$,
 where $I_{i \in S_o} \sim \text{Bern}(p)$
- 3: Construct condition c such that

$$c_i = \begin{cases} x_i, & \text{if } i \in S_o \\ 0, & \text{otherwise} \end{cases}$$

- 4: Diffusion step with target x and condition c
 - 5: **end for**
-

This training procedure implicitly defines an amortized conditional learning objective:

$$\mathbb{E}_{c \sim P(c)} \mathbb{E}_{t, x_0, \epsilon} [\|\epsilon - \epsilon_\theta(x_t, t, c)\|^2] \quad (5)$$

where $p(c), c \in \mathcal{C}$ is the distribution of conditional configuration (i.e. combinations of observable channels) over the conditional space \mathcal{C} . Therefore, one can treat the random masking training as an amortized inference over the condition space. Minimizing eq. (5) encourages the model to learn a single amortized estimator $\epsilon_\theta(x_t, t, c)$ such that $\epsilon_\theta(x_t, t, c) \approx \nabla_{x_i} \log p(x_t | c)$ for arbitrary condition c . This strategy relies on the assumption that partially observed structured data can provide informative gradients in amortized training. Although not formally addressed, previous work has shown its effectiveness in various domains [11, 12], and we provide empirical justification in section 5.2.

3.3 Channel Attention for Structured Feature Modulation

With random channel masking, our model aims to handle arbitrary conditional configurations, where the observed channels may vary across samples and tasks. Since all condition c are encoded with the same conditional network, the model needs to adaptively select and reweight latent features depending on the conditions. To enable the model to dynamically recalibrate features in both latent and data space, we introduce a bespoke channel-wise attention module in each UNet block (fig. 2a). We consider two designs, each focusing on distinct modeling goals.

The first is a lightweight attention mechanism inspired by the Squeeze-and-Excitation (SE) network [13]. Given a latent feature map $z \in \mathbb{R}^{D \times H \times W}$, we compute

$$\begin{aligned} \alpha &= \text{GAP}(z) \\ w &= \sigma(W_2 \cdot \phi(W_1 \cdot \alpha)) \\ z' &= w \cdot z \end{aligned} \quad (6)$$

where ϕ is a non-linearity (e.g., ReLU), GAP stands for global average pooling, and σ is the sigmoid function. This approach scales each latent channel by a learned weight conditioned on the global context and enables a per-sample feature reweighting that aligns with the dynamic feature selection requirement for the random channel masking.

Alternatively, we can perform a full channel-wise self-attention across all channels:

$$x_{\text{flat}} \in \mathbb{R}^{D \times N}, \quad N = H \times W, \quad Q = x_{\text{flat}} W_Q, \quad K = x_{\text{flat}} W_K, \quad V = x_{\text{flat}} W_V \quad (7)$$

$$A = \text{softmax} \left(\frac{QK^\top}{\sqrt{d}} \right), \quad x'_{\text{flat}} = AV \quad (8)$$

Compared to SE channel attention, this design is more expressive and can capture higher-order dependencies among channels. This feature makes the transformer-based channel attention particularly useful within the UNet blocks, where the model infers the missing information across latent features.

We introduce an additional channel attention mechanism at the final stage of the model, operating over the semantic output channels. Let the final latent representation before projection be $z \in \mathbb{R}^{D \times H \times W}$, where D is the number of latent channels. The standard diffusion model produces $\hat{y} \in \mathbb{R}^{C \times H \times W}$ with a single output layer. To model cross-channel dependencies, we add an additional layer that computes

$$\hat{y}_{\text{attn}} = y + \text{Conv1}(\text{SE}(y)) \quad (9)$$

Together, these two attention modules allow the model to modulate features both within the latent space and across semantic output channels, improving performance on tasks involving complex, structured channel relationships.

4 Related Work

Image inpainting with conditional diffusion models. Recent work has applied diffusion-based generative models to image inpainting and completion tasks [5, 6]. These models primarily work on natural and grayscale images, where the number of channels is limited ($n \leq 3$), and the goal is to reconstruct spatially masked regions based on the surrounding context. These models often take conditionals like class labels [14], text embeddings [15, 16], or segmentation maps [1]. These conditionals are typically injected via concatenation at the input or embedding injection via FiLM modulation. This approach ignores the implicit spatial alignment between the conditionals and the generative target. More recent approaches like ControlNet [2] and BrushNet [7] introduce multiscale conditioning mechanisms that are spatially aligned and applied post hoc to pre-trained Stable Diffusion models. While these methods preserve spatial alignment, they assume low-dimensional RGB-style inputs with simple spatial masks and do not address the challenges posed by high-dimensional structured data with intricate inter-channel dependencies. Moreover, because their conditioning modules are trained separately from the core generative model, they lack end-to-end coordination between condition encoding and generation.

Dynamic guidance for conditional diffusion. Classifier-free guidance (CFG) [17] introduces a flexible training scheme for conditional diffusion models by randomly dropping conditioning inputs and jointly training the model on both conditional and unconditional objectives. While originally developed for low-dimensional conditioning signals such as class labels, the core idea can be generalized: using input masking during training to enable flexible guidance at test time. We adopt this principle in the form of random-masking guidance, where the spatial conditions are randomly masked during training. Specifically, the model observes a random subset of input channels and is trained to reconstruct the full panel. This dynamic masking encourages the model to learn a unified generative model that generalizes across different conditionals, making it suitable for tasks where the available condition varies across samples. This approach enables multi-channel prediction and supports generation under arbitrary conditioning subsets without retraining or architectural changes.

Channel-aware attention mechanisms. While channel-wise attention has been explored in vision architectures like SENet [13], most diffusion-based models focus on spatial attention and overlook channel-wise relationships. However, this becomes a significant limitation in multi-channel biological data. A few recent works in diffusion-based colorization have begun to explore this direction: FCNet [18] introduces spatially decoupled color representations tailored to facial regions, and ColorPeel [19] learns disentangled geometric shapes and color embeddings in latent space. These models can be thought of as coarse region-level attention over RGB channels and are not designed for tasks involving dozens or hundreds of semantically distinct channels.

Table 1: Benchmarking our multimodal diffusion approach against existing modality prediction methods on gene-to-protein prediction task on four (PBMC, CBMC, BMNC and HSPCs) datasets. r_c shows the cell-wise correlation with the ground truth, and r_p shows the protein-level correlation.

Method	PBMC		CBMC		BMNC		HSPC	
	r_c	r_p	r_c	r_p	r_c	r_c	r_p	r_c
KRR [26]	0.908	0.646	0.863	0.006	0.870	0.094	0.820	0.059
MultiVI [28]	0.088	0.069	0.103	0.032	0.082	0.054	0.045	0.035
GLUE [29]	0.659	-0.004	0.623	0.054	0.589	0.012	0.549	0.024
UnitedNet [21]	0.870	0.518	0.377	0.628	0.625	0.634	0.310	0.436
scMM [20]	0.793	0.521	0.736	0.517	0.853	0.625	0.724	0.598
Ours (500 steps)	0.880	0.673	0.962	0.763	0.879	0.685	0.865	0.647
Ours + SiD (1 step)	0.874	0.672	0.962	0.759	0.875	0.682	0.865	0.642

Structured image generation in science. Generative models for scientific data, such as multiplexed tissue imaging and spatial transcriptomics, have primarily relied on deterministic architectures, including CNNs and transformers. A few recent methods have extended probabilistic modeling to single-cell multi-omics prediction (e.g., scMM [20], UnitedNet [21]) or protein inference from gene expression [22], but do not leverage generative diffusion frameworks. The most recent Stem [23] incorporates diffusion models (specifically DiT) for spatial transcriptomics. However, Stem conditions only on vector embeddings of RGB histology images that break the spatial alignment, and does not account for inter-channel relationships in the generated modalities. Our work builds on these directions by introducing a controllable diffusion-based model tailored to biological profiling data with structured, multi-channel inputs.

5 Experiments

We evaluate our model on both single-cell and spatial imaging datasets to test its capacity for conditional multi-channel generation across modalities, tissues, and prediction modes. Our experiments are designed to test (1) prediction performance against state-of-the-art methods, (2) the ability to model inter-channel relationships in multi-channel spatial data, (3) generalization to unseen channel configurations, (4) cross-dataset generalizability, and (5) the contribution of each model component. We report Pearson correlation (r) between predicted and ground truth channels unless otherwise specified.

5.1 Single-cell modality prediction

We first benchmark our model on the task of predicting protein expression from scRNA-seq profiles, a standard benchmark in single-cell multimodal modeling. We use four publicly available datasets: peripheral blood mononuclear cells (PBMC) [24], cord blood mononuclear cells (CBMC) [25], bone marrow mononuclear cells (BMMC) [26] and hematopoietic stem and progenitor cells (HSPCs) [27]. Each dataset contains paired single-cell gene expression (mRNA) and surface protein (ADT) measurements.

We train the model to predict all protein channels from full gene expression vectors. We compare to a suite of state-of-the-art methods: Kernel Ridge Regression [26], MultiVI [28], GLUE [29], scMM [20], and UnitedNet [21]. Performance is reported as average Pearson correlation between predicted and measured expression levels across proteins (r_p) and cells (r_c). Table 1 shows that our model consistently outperforms all baselines across all four CITE-seq datasets. In particular, our model achieves the highest protein-level correlation r_p , which is the more biologically relevant metric, in each setting. We further evaluated the performance of a distilled version of our model capable of performing fast, 1-step inference (via SiD [30, 31]). Our method remains competitive with 1-step distillation, suggesting it can be readily deployed for use by biologists with low overhead.

5.2 Spatial protein imputation

Single channel imputation. To evaluate the model’s performance in spatial contexts, we apply it to high-dimensional tissue images from Imaging Mass Cytometry (IMC), where each pixel corresponds

Table 2: Comparison of predictive correlation across different methods in spatial prediction tasks. Our method outperforms the diffusion, single-protein, and linear baselines, and diffusion based ControlNet [2], domain-specific models like Stem [23] and MULTIPLAI [22].

Method	Breast	Lung
Most correlated protein	0.489	0.506
Most spatially correlated protein	0.581	0.627
MULTIPLAI [22]	0.353	0.349
Stem [23]	0.403	0.475
ControlNet [2]	0.452	0.537
Ours (single channel)	0.667	0.703
Ours (multi channel)	0.596	0.647

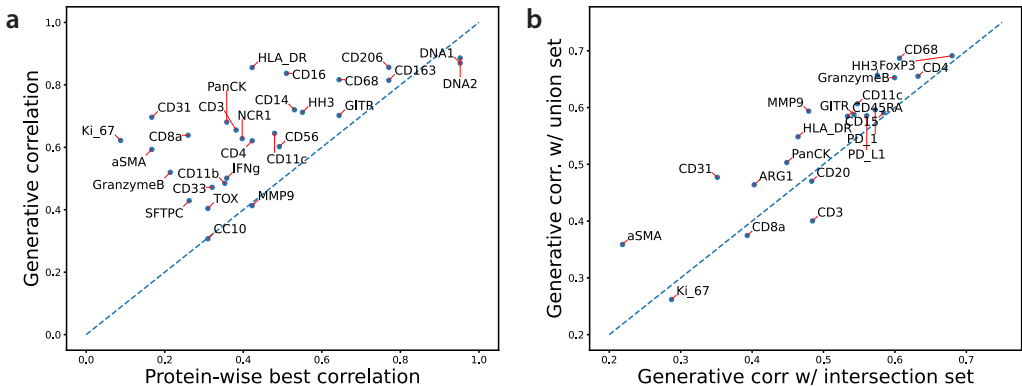


Figure 3: (a) Benchmarking generative performance (Pearson’s r) against the most similar protein on the lung cancer dataset. (b) Cross-dataset generalization study results. Using the union of all protein channels, even those missing from the test dataset, consistently outperforms using only the overlapping set of protein channels.

to spatially co-registered multi-protein expression signals. We evaluate our method on two IMC datasets: a lung cancer cohort [32] (8 patients) and a breast cancer cohort [33] (6 patients), with 43 and 50 co-registered protein channels, respectively. Images are normalized per channel and tiled into to 64×64 patches, which is further decreased to 16×16 by pretrained encoder. We compare our method to two simple baselines, single-protein predictor and kernel ridge regression, and structured conditional diffusion models, ControlNet [2]. We also include domain-specific methods, STEM [23] and MULTIPLAI [22]. For each image, in the single channel prediction setup, we mask one protein channel at a time as the target and use the rest as the spatial condition.

Table 2 shows our method outperforms all existing approaches on both IMC datasets. All baseline models fail to outperform the best linear predictor and most fail to outperform the best individual observed protein feature. In the Appendix, we also present hybrid experiments comparing two diffusion models (ControlNet and BrushNet [7]) augmented with elements of our proposed model; results show these methods still do not outperform our full method. This highlights how, unlike in natural RGB images, the spatial structure in biological models presents fundamental challenges to standard diffusion models. By contrast, our method consistently performs better than the baselines across each individual protein channel, sometimes by more than 300% (See fig. 3a for the performance of the multi-channel model). Fixing the channel known to be missing during training improves performance in the single-protein prediction mode, but the multi-channel prediction model that learns all channels jointly still achieves better performance than any baseline. Section 1 shows qualitative reconstructions of proteins. These results validate the effectiveness of random-masking guidance and support practical use cases where multi-channel prediction is required.

Table 3: Ablation studies with 4 different architectural setups on the breast cancer dataset; test score is the average over all proteins.

Method	r
Best Protein Predictor	0.489
Single channel	0.667
Multi channel	0.596
w/o output channel attention	0.581
w/o UNet channel attention	0.541
Condition injection w/ element-wise addition	0.516
Condition injection w/ channel attention	0.535
Base (unconditional)	-0.017

Cross-dataset generalization. We further test our model’s ability to learn from datasets with partially overlapped protein channels. Specifically, we combine the lung and breast cancer IMC datasets. The two datasets have 23 proteins in common, with 18 unique lung panel proteins and 21 unique breast panel proteins. We evaluate our model under two training schemes: (1) an intersection setting, where we keep only the proteins observed in both datasets and (2) a union setting, where we include the union of all protein channels and zero-pad missing channels in each dataset. Both setups share the same model architecture and training strategy with random masking, and both predict the intersection set at test time.

As shown in fig. 3b, the union setup consistently outperforms the intersection counterpart, achieving a higher average Pearson correlation in sample generation. Although increasing the sparsity of supervision, the union setup has a broader coverage and enables the model to learn a richer set of inter-channel dependencies and improves its robustness to missing data. The model effectively leverages partially observed data and maintains performance by training on the union of proteins with zero-padded missing channels. Structurally aligned but partially missing data can still carry informative gradients for joint learning under random-masking guidance, highlighting random-masking guidance as a principled method for multi-dataset integration with empirical advantages.

5.3 Ablation studies

We conduct ablation experiments to disentangle the contributions of each architectural component. Using the lung cancer IMC dataset, we compare two feature injection mechanisms: elementwise addition and soft channel-wise attention, as well as three attention configurations: (1) with channel-wise attention only in the UNet blocks, (2) with channel-wise attention only in the output block, and (3) the full model combining both mechanisms.

Table 3 summarizes the contributions of each architectural component. The unconditional baseline performs poorly, with Pearson $r < 0.1$. Adding hierarchical feature injection significantly improves performance, and conditional injection via soft channel attention further improves over conventional element-wise addition. Output-space channel attention provides modest gains, while latent-space channel attention leads to more substantial improvements, capturing complex inter-channel dependencies in the latent feature space. These results support integrating both spatially aligned conditioning and channel-wise attention for multi-channel imputation.

6 Conclusion

We introduced a diffusion-based generative model for controllable generation of multi-channel biological profiling data, capable of handling arbitrary combinations of observed and missing modalities. Biological profiling technologies such as IMC and 10X Xenium [34] are expensive, time-consuming, and require specific panel design, which can only cover a subset of the total molecules of interest at a time. These constraints limit the scientific utility of these technologies. Our controllable generative model offers an *in silico* extension to the pre-designed profiling panel, and has the potential to recover corrupted or incomplete acquisitions. The ability of our model to learn rich priors over distinct tissue types and microenvironments suggests it may make a strong basis for a foundation model for

spatial biology. In future work, we plan to explore scaling our model to dozens or hundreds of spatial datasets to enable broad protein channel imputation.

References

- [1] Robin Rombach, Andreas Blattmann, Dominik Lorenz, Patrick Esser, and Björn Ommer. High-resolution image synthesis with latent diffusion models. In *Proceedings of the IEEE/CVF Conference on Computer Vision and Pattern Recognition*, pages 10684–10695, 2022.
- [2] Lvmin Zhang, Anyi Rao, and Maneesh Agrawala. Adding conditional control to text-to-image diffusion models. In *ICCV*, 2023.
- [3] Qing Chang, Olga I Ornatsky, Iram Siddiqui, Alexander Loboda, Vladimir I Baranov, and David W Hedley. Imaging mass cytometry. *Cytometry Part A*, 91(2):160–169, 2017.
- [4] Lambda Moses and Lior Pachter. Museum of spatial transcriptomics. *Nature Methods*, 19(5):534–546, 2022.
- [5] Yang Song and Stefano Ermon. Generative modeling by estimating gradients of the data distribution. In *Advances in Neural Information Processing Systems (NeurIPS)*, volume 33, pages 11895–11907, 2020.
- [6] Chitwan Saharia, William Chan, Huiwen Chang, Chris A. Lee, Jonathan Ho, Tim Salimans, David Fleet, and Mohammad Norouzi. Palette: Image-to-image diffusion models. 2022.
- [7] Xuan Ju, Xian Liu, Xintao Wang, Yuxuan Bian, Ying Shan, and Qiang Xu. Brushnet: A plug-and-play image inpainting model with decomposed dual-branch diffusion. In *CVPR*, 2024.
- [8] Jascha Sohl-Dickstein, Eric A. Weiss, Niru Maheswaranathan, and Surya Ganguli. Deep unsupervised learning using nonequilibrium thermodynamics. In *Proceedings of the 32nd International Conference on Machine Learning (ICML)*, volume 37, pages 2256–2265, 2015.
- [9] Jonathan Ho, Ajay Jain, and Pieter Abbeel. Denoising diffusion probabilistic models. In *Advances in Neural Information Processing Systems*, 2020.
- [10] Tony F Chan and Jianhong Shen. Nontexture inpainting by curvature-driven diffusions. *Journal of visual communication and image representation*, 12(4):436–449, 2001.
- [11] Samuel Gershman and Noah Goodman. Amortized inference in probabilistic reasoning. In *Proceedings of the annual meeting of the cognitive science society*, volume 36, 2014.
- [12] Joe Marino, Yisong Yue, and Stephan Mandt. Iterative amortized inference. In *International Conference on Machine Learning*, pages 3403–3412. PMLR, 2018.
- [13] Jie Hu, Li Shen, and Gang Sun. Squeeze-and-excitation networks. In *Proceedings of the IEEE Conference on Computer Vision and Pattern Recognition*, pages 7132–7141, 2018.
- [14] Prafulla Dhariwal and Alex Nichol. Diffusion models beat gans on image synthesis. In *Advances in Neural Information Processing Systems*, volume 34, pages 8780–8794, 2021.
- [15] Aditya Ramesh, Prafulla Dhariwal, Alex Nichol, Casey Chu, and Mark Chen. Hierarchical text-conditional image generation with clip latents. *arXiv preprint arXiv:2204.06125*, 2022.
- [16] Alex Nichol, Prafulla Dhariwal, Aditya Ramesh, Pranav Shyam, Pamela Mishkin, Bob McGrew, Ilya Sutskever, and Mark Chen. Glide: Towards photorealistic image generation and editing with text-guided diffusion models. 2022.
- [17] Jonathan Ho and Tim Salimans. Classifier-free diffusion guidance. In *NeurIPS 2021 Workshop on Deep Generative Models and Downstream Applications*, 2021.
- [18] Kai Zhang, Jiaxin Huang, Yujie Zhong, Yifan Sun, Jing Li, and Jiebo Luo. Learning spatially decoupled color representations for facial image colorization. *arXiv preprint arXiv:2304.12345*, 2024.

- [19] Muhammad Atif Butt, Kai Wang, Javier Vazquez-Corral, and Joost van de Weijer. Colorpeel: Color prompt learning with diffusion models via color and shape disentanglement. 2024.
- [20] Kodai Minoura, Ko Abe, Hyunha Nam, Hiroyoshi Nishikawa, and Teppei Shimamura. A mixture-of-experts deep generative model for integrated analysis of single-cell multiomics data. *Cell Reports Methods*, 1(5):100071, 2021.
- [21] Xin Tang, Jiawei Zhang, Yichun He, Xinhe Zhang, Zuwan Lin, Sebastian Partarrieu, Emma Bou Hanna, Zhaolin Ren, Hao Shen, Yuhong Yang, Xiao Wang, Na Li, Jie Ding, and Jia Liu. Explainable multi-task learning for multi-modality biological data analysis. *Nature Communications*, 2024.
- [22] Javier Martin-Gonzalez et al. Predictive modeling of highly multiplexed tumor tissue images by graph neural networks. *medRxiv*, 2021.
- [23] Sichen Zhu, Yuchen Zhu, Molei Tao, and Peng Qiu. Diffusion generative modeling for spatially resolved gene expression inference from histology images. In *International Conference on Learning Representations (ICLR)*, 2025.
- [24] Yuhan Hao, Stephanie Hao, Erica Andersen-Nissen, William M Mauck, Shiwei Zheng, Andrew Butler, Maddie J Lee, Aaron J Wilk, Charlotte Darby, Michael Zager, et al. Integrated analysis of multimodal single-cell data. *Cell*, 184(13):3573–3587, 2021.
- [25] Marlon Stoeckius, Christoph Hafemeister, William Stephenson, Brian Houck-Loomis, Pratip K Chattopadhyay, Harold Swerdlow, Rahul Satija, and Peter Smibert. Simultaneous epitope and transcriptome measurement in single cells. *Nature methods*, 14(9):865–868, 2017.
- [26] Christopher Lance, Malte D. Luecken, Daniel B. Burkhardt, Robrecht Cannoodt, Pia Rautenstrauch, Anna Laddach, Aidyn Ubingazhibov, Zhi-Jie Cao, Kaiwen Deng, Sumeer Khan, Qiao Liu, Nikolay Russkikh, Gleb Ryazantsev, Uwe Ohler, NeurIPS 2021 Multimodal data integration competition participants, Angela Oliveira Pisco, Jonathan Bloom, Smita Krishnaswamy, and Fabian J. Theis. Multimodal single cell data integration challenge: Results and lessons learned. In *Proceedings of the NeurIPS 2021 Competitions and Demonstrations Track*, volume 176, pages 162–176, 2022.
- [27] Sonia Nestorowa, Fiona K Hamey, Blanca Pijuan Sala, Evangelia Diamanti, Mairi Shepherd, Elisa Laurenti, Nicola K Wilson, David G Kent, and Berthold Göttgens. A single-cell resolution map of mouse hematopoietic stem and progenitor cell differentiation. *Blood, The Journal of the American Society of Hematology*, 128(8):e20–e31, 2016.
- [28] Tal Ashuach, Mariano I. Gabitto, Rohan V. Koodli, Giuseppe-Antonio Saldi, Michael I. Jordan, and Nir Yosef. Multivi: deep generative model for the integration of multimodal data. *Nature Methods*, 2023.
- [29] Zhi-Jie Cao and Ge Gao. Multi-omics single-cell data integration and regulatory inference with graph-linked embedding. *Nature Biotechnology*, 40, 2022.
- [30] Mingyuan Zhou, Huangjie Zheng, Zhendong Wang, Mingzhang Yin, and Hai Huang. Score identity distillation: Exponentially fast distillation of pretrained diffusion models for one-step generation. In *Proceedings of the 41st International Conference on Machine Learning*, 2023.
- [31] Mingyuan Zhou, Xiaoyong Yuan, Fengyu Yang, Weixin Chen, Jinghui Chen, and Qiang Liu. Adversarial score identity distillation: Rapidly surpassing the teacher in one step. *arXiv preprint arXiv:2410.14919*, 2024.
- [32] Liron Yoffe, Bhavneet Bhinder, Sung Wook Kang, Haoran Zhang, Arshdeep Singh, Hiranmayi Ravichandran, Geoffrey Markowitz, Mitchell Martin, Junbum Kim, Chen Zhang, et al. Acquisition of discrete immune suppressive barriers contributes to the initiation and progression of preinvasive to invasive human lung cancer. *bioRxiv*, pages 2024–12, 2025.
- [33] Hartland W Jackson, Jana R Fischer, Vito RT Zanotelli, H Raza Ali, Robert Mechera, Savas D Soysal, Holger Moch, Simone Muenst, Zsuzsanna Varga, Walter P Weber, et al. The single-cell pathology landscape of breast cancer. *Nature*, 578(7796):615–620, 2020.

- [34] Amanda Janesick, Robert Shelansky, Andrew D Gottscho, Florian Wagner, Stephen R Williams, Morgane Rouault, Ghezal Beliakoff, Carolyn A Morrison, Michelli F Oliveira, Jordan T Sicherman, et al. High resolution mapping of the tumor microenvironment using integrated single-cell, spatial and in situ analysis. *Nature Communications*, 14(1):8353, 2023.